

Incorporation of Decavanadate Ions into Silica Gels and Mesostructured Silica Walls

Hyuk Choi, Yoon-Young Chang, and Young-Uk Kwon*

Department of Chemistry and BK-21 School of Molecular Science,
Sungkyunkwan University, Suwon, 440-746, Korea

Oc Hee Han*

Solid-State Analysis Team, Daegu Branch, Korea Basic Science Institute and Department of
Industrial Chemistry, Kyungpook National University, Daegu, 702-701, Korea

Received February 16, 2003. Revised Manuscript Received May 14, 2003

Decavanadate ($V_{10}O_{28}^{6-}$) polyoxometalate (POM) ions in water decompose into smaller POM ions or monomeric $H_2VO_4^-$ when the pH is raised to higher than 6. In this report, however, we have found that silicate ions can kinetically stabilize decavanadate ions for up to 8 h at pH 12 conditions. Gelation of these solutions by lowering the pH to 4–5 followed by aging produced monolithic vanadia–silica composite gels with a wide range of vanadium contents ($V/(V + Si)$ up to 48%). Solid state ^{51}V NMR and infrared spectroscopic data show that the vanadium species is predominantly $V_{10}O_{28}^{6-}$ when the vanadium content is $2.3\% \leq V/(V + Si) \leq 32\%$ and another $V(V)$ species in distorted octahedral coordination starts to appear in addition to $V_{10}O_{28}^{6-}$ for high vanadium content of $V/(V + Si) = 48\%$. The kinetic stabilization of decavanadate by silicate ions suggests that the silicate ions condense around the decavanadate ions to form a core–shell like structure that may behave as pure silica in some chemical reactions. Thus, upon processing as in the synthesis of mesoporous silica using a cationic surfactant myristyltrimethylammonium bromide we have synthesized hexagonal mesostructured materials with vanadia–silica composite walls.

Introduction

There have been many reports on the synthesis of homogeneous multicomponent materials that may find applications such as catalysts, optical materials, sensors, and ionic conductors.^{1,2} Mainly by using sol–gel chemistry in alcohol solutions, various types of homogeneous gels have been achieved including aerogels and xerogels.³ Of these, the vanadia–silica system is one of the most extensively studied in which homogeneous dispersion and high loading of vanadium atoms in the silica matrixes have been the major issues, and vanadium content up to 14.1% has been reported.⁴ Beyond this limit, the vanadium species tend to form V_2O_5 and phase-separate to produce inhomogeneous mixtures. The vanadia–silica gel is commonly obtained by acid-catalyzed hydrolysis reactions of silica. In these processes, it is hard to control the vanadia species because

of vanadium reduction by the acid catalyst and the formation of various polymeric vanadium species upon concentration.

The reported mixed vanadia–silica materials (silicalite, co-gel, and silica supported) are all constituted of monomeric or dimeric vanadate species dispersed in the silica frameworks.⁵ The atomic and structural features of a hybrid xerogel in which discrete vanadium oxide units exist in a silica matrix have been recently reported by Stiegman et al.⁶

In the present study, we have taken a different approach using decavanadate ($V_{10}O_{28}^{6-}$) ions (Figure 1) as the starting material. This study stems from our pursuit to synthesize composite materials by using polyoxometalate (POM) ions.⁷ The identities and predominance of various vanadate species in aqueous solutions as a function of pH and vanadium concentration have been well elucidated by previous ^{51}V NMR studies.⁸ Decavanadate is the largest vanadate cluster and is predominant between pH 3 and 6 at concentra-

* Authors to whom correspondence should be addressed. Y.-U.K. Phone: 82-31-290-7070. Fax: 82-31-290-7075. E-mail: ywkwon@chem.skku.ac.kr. O.H.H. Phone: 82-53-950-7912. E-mail: ohhan@kbsi.re.kr.

(1) Kundu, D.; Biswas, P. K.; Ganguli, G. *J. Non-Cryst. Solids* **1989**, 110, (b) Dave, B. C.; Dunn, B.; Valentine, J. S.; Zink, J. I. *Anal. Chem.* **1994**, 66, 1120. (c) Badini, G. E.; Grattan, K. T. V.; Tseung, A. C. C. *Rev. Sci. Instrum.* **1995**, 66, 4034. (d) Ghosh, A.; Chakravorty, D. *Appl. Phys. Lett.* **1991**, 59, 855. (e) McCulloch, S.; Stewart, R. M.; Guppy, R. M.; Norris, J. O. W. *Int. J. Optoelectron.* **1994**, 9, 235.

(2) Stiegman, A. E.; Eckert, H.; Plett, G.; Kim, S.-S.; Anderson, M.; Yavorouian, A. *Chem. Mater.* **1993**, 5, 1591.

(3) Brinker, C. J.; Scherer, G. W. *Sol–Gel Science*; Academic Press: San Diego, CA, 1990.

(4) Curran, M. D.; Gedris, T. E.; Stiegman, A. E. *Chem. Mater.* **1999**, 11, 1120.

(5) Wang, C. B.; Deo, G.; Wachs, I. E. *J. Catal.* **1998**, 178, 640.

(6) Tran, K.; Hanning-Lee, M. A.; Biswas, A.; Stiegman, A. E.; Scott, G. W. *J. Am. Chem. Soc.* **1995**, 117, 2618.

(7) Choi, H.; Kwon, Y.-U.; Han, O.-H. *Chem. Mater.* **1999**, 11, 1641. (b) Son, J.-H.; Choi, H.; Kwon, Y.-U. *J. Am. Chem. Soc.* **2000**, 122, 7432. (c) Son, J.-H.; Kwon, Y.-U. *Bull. Kor. Chem. Soc.* **2001**, 22, 1224. (d) Son, J.-H.; Choi, H.; Kwon, Y.-U.; Han, O. H. *J. Non-Cryst. Solids* **2003**, 318, 186. (e) Son, J. H.; Kwon, Y.-U.; Han, O. H. *Inorg. Chem.* **2003**, 42, 4153.

(8) Howarth, O. W.; Jarrold, M. *J. Chem. Soc., Dalton Trans.* **1978**, 503. (b) Heath, E.; Howarth, O. W. *J. Chem. Soc., Dalton Trans.* **1981**, 1105.

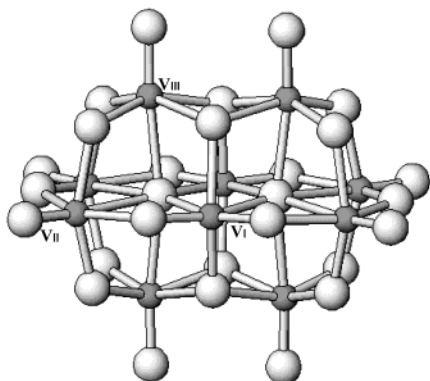


Figure 1. Structure of decavanadate ($V_{10}O_{28}^{6-}$) anion. Small filled circles represent vanadium atoms and large open circles represent oxygen atoms. Three different vanadium nuclei of chemically equivalent sites are marked as V_I , V_{II} , and V_{III} .

tions in excess of 0.01 M V^{5+} . We have found that the use of the decavanadate clusters in synthesizing multi-component materials gives an advantage in achieving high vanadium loading because of the clustering of vanadium atoms.

Several POM-loaded silica materials already have been reported, mainly with tungsten-based POMs. $SiW_{12}O_{40}^{4-}$, $PW_{12}O_{40}^{4-}$, and $W_{12}O_{32}^{4-}$ were incorporated into silica matrices via the sol-gel method and these materials exhibit catalytic and antistatic properties, and photocatalytic activity.^{9–11} Molybdenum-based POM-silica hybrid materials were reported recently for their potential catalytic properties.¹² On the other hand, there is no example of POMs of other metal atoms such as vanadium. This is probably due to the narrow pH window for the stability of other POMs whereas the tungsten and molybdenum POMs are stable at pH 0–6 in which region most sol-gel reactions of the matrix silica materials are performed.

In the latter part of this paper, we report surfactant-templated synthesis of mesostructured and mesoporous materials with vanadia-silica composite walls. Many researchers have tried to incorporate transition metal atoms into the pores of mesoporous silica for catalytic applications.¹³ However, there are only a few papers that describe mesoporous materials with composite walls.¹⁴ In this regard, the synthesis method of mesoporous materials of vanadia-silica composite walls of this paper will contribute to the development of a potentially important class of catalyst materials.

Experimental Section

Synthesis of Vanadia-Silica Monolithic Gels. A decavanadate solution was prepared by dissolving sodium metavanadate in deionized water (18.0 M Ω /cm) to make $[V] = 0.3$ M and adding a 2 M HCl solution until pH = 4.5. This solution

was diluted to various vanadium concentrations by adding deionized water, and the pHs of these diluted solutions were readjusted to ca. 4.5 with a 0.2 M HCl solution to get orange-colored solutions. These solutions were kept for 48 h and then the pH was readjusted to ca. 4.5 to ensure complete equilibrium so that the predominant species was the decavanadate ion. A 2.6 mL (16 mmol) portion of a sodium metasilicate solution (Aldrich; 14% NaOH, 27% SiO_2) was added to each of the decavanadate solutions (50 mL) with stirring. In this way, solutions of compositions $V/(V + Si) = 2.3, 4.4, 19, 32,$ and 48% were prepared; these will be named by their vanadium contents, as in VSi19. The pH of these solutions rose to ca. 11.5–12.3. The pH rise of VSi48 solution is slightly lower than that of VSi2.3 because of the higher decavanadate content. After 1 h of stirring, a 2 M HCl solution was slowly added to reach pH 4.5 to induce acid-catalyzed gelation of silicate ions. The solutions were homogeneous, transparent, and orange throughout the procedure. These solutions were aged at 86 °C for 18 h in a drying oven. The gelation began to occur on the solution surface after 2 h and progressed inwardly with volume contraction due to water evaporation. The gelation becomes faster with the increase of the decavanadate content. The obtained gel samples were dried in an evacuated desiccator at room temperature. A vanadium-free silicate gel (VSi0.0) as a reference was also prepared by the same procedure but without vanadium included.

Synthesis of Mesostructured Materials with Vanadia-Silica Composite Walls. Mesostructured materials with vanadia-silica wall materials were synthesized using silicate-stabilized decavanadate solutions of the VSi32 or VSi48 compositions and myristyltrimethylammonium bromide ($(CH_3(CH_2)_{13}N(CH_3)_3Br$, MTAB) as a template. Typically, to 25 mL of a solution of VSi48 composition at pH 11.5, 2.39 g of MTAB was added to make the composition $SiO_2/MTAB/NaVO_3/H_2O$ 1:0.86:0.92:176. A yellow precipitate formed immediately. A 2 M HCl solution was added to adjust the pH to 4.5–8. The resultant mixtures were rapidly stirred at room temperature for 12 h and aged for 2–3 days at 80 °C in an oven. The precipitates were filtered, washed, and vacuum-dried, and UV-irradiated (254 nm) for 27 h to remove the organic template molecules.¹⁵

⁵¹V Solution NMR Spectroscopy. ⁵¹V solution NMR spectra of the decavanadate-silicate mixed solutions before gelation were obtained by Varian Unity Inova 500 MHz spectrometer using a 10-mm broad-band probe tuned to 131.5 MHz for ⁵¹V nucleus. Data were collected over an 84745.8 Hz sweep width with an acquisition time of 0.524 s and recycle delay of 1 s using a 45° excitation pulse. The line broadening of 10 Hz was applied prior to Fourier transformation. All chemical shifts were measured at ambient temperature and externally referenced to neat $VOCl_3$ liquid (0 ppm).

⁵¹V Solid State NMR Spectroscopy. The magic angle spinning (MAS) ⁵¹V solid-state NMR spectra of the gel samples were acquired on a Bruker DSX 400 spectrometer with Larmor frequency of 105.19 MHz. The spectra with spinning speed of 13 kHz are shown in this work, however, various spinning rates were employed to check the center peaks when necessary. All chemical shifts were referenced against neat $VOCl_3$ liquid by using saturated $NaVO_3$ aqueous solution (–578 ppm).

Other Characterizations. Thermogravimetric analysis was performed on a TA4000/SDT2960 thermogravimetric analyzer. The gel samples were placed in a platinum crucible and dried by air purging for 30 min to reduce possible errors from different degrees of drying, and were heated to 1000 °C at a heating rate of 5 °C/min in an air flow of 100 mL/min. Infrared spectra were recorded from ground gel samples with the KBr method using a Nicolet 205 FT-IR spectrometer. 150 scans were accumulated for each spectrum in the transmission mode at a spectral resolution of 2 cm^{-1} . The low-angle X-ray diffraction patterns of the mesostructured materials were obtained by a RIGAKU D/max-RC powder X-ray diffractometer (Cu $K\alpha$ radiation) in the 2θ range of 1–5°. Transmission

(9) Judeinstein, P.; Schmidt, H. *J. Sol-Gel Sci. Technol.* **1994**, *3*, 189.

(10) Minami, N.; Hiraoka, M.; Izumi, K.; Uchida, Y. Japanese Patent JP 08113732 A2, 1996; *Chem. Abstr.* **1996**, *125*, 117543. (b) Minami, N.; Hiraoka, M.; Izumi, K.; Uchida, Y. Japanese Patent JP 08141493 A2, 1996; *Chem. Abstr.* **1996**, *125*, 171066.

(11) Ozer, R. R.; Ferry, J. L. *Environ. Sci. Technol.* **2001**, *35*, 3242.

(12) Polarz, S.; Smarsly, B.; Goltner, C.; Antioietti, M. *Adv. Mater.* **2000**, *12*, 1503.

(13) Trong On, D.; Desplandier-Giscard, D.; Danumah, C.; Kaliaquine, S. *Applied Catal. A: General* **2001**, *222*, 299.

(14) Luca, V.; Maclachlan, D. J.; Morgan, K. *Chem. Mater.* **1997**, *9*, 2720.

(15) Keene, M. T. J.; Denoyel, R.; Llewellyn, P. L. *Chem. Commun.* **1998**, *20*, 2203.

electron microscopic images of the UV-treated mesostructured materials were obtained using a JEOL-3011 model operating with a 300-kV electron beam.

Results and Discussion

The predominant vanadium species in an aqueous system is changed in the order $V_{10}O_{28}^{6-}$, $V_4O_{12}^{4-}$, $V_2O_7^{4-}$, and VO_4^{3-} as the solution pH increases from 4 to 12.¹⁶ Normally, the decavanadate ions are decomposed into the smaller vanadium oxoanions within 2 h by raising the pH to 11–12. This reaction is easy to follow visually because the decavanadate ions are deep orange while the tetramers are light yellow and the monomers and dimers are colorless. Contrary to this moderately fast decomposition reaction in the unitary vanadium solution, when the pH was raised to 11–12 by adding a metasilicate solution, the solutions maintained their orange color for up to 8 h. The decoloration may be facilitated by vigorous stirring. These observations suggest that the decavanadate ions are kinetically stabilized by the silicate species despite the unfavorably high pH. Although it is not clear how the decavanadate ions are stabilized by the silicate species at the high pH condition, we believe that the materials have a core-shell like structure with the decavanadate ion in the core and (loosely) condensed silicate ions in the shell, and the negatively charged core and shell are held by sodium ions between them. The silica shell acts as a diffusion barrier for OH^- ions that, otherwise, would induce the decomposition of the decavanadate ion in the core. The presence of the “linker” sodium ion layer between the decavanadate core and the silicate shell is very likely in view of the reported high association constant between decavanadate and sodium ions in solutions,¹⁷ and the crystal structures of decavanadate compounds that show direct interactions between decavanadate and sodium ions.¹⁸

Therefore, when the solution pH was lowered again to 4.5 by adding a HCl solution after being kept at pH 11–12 for 1 h, the solution was still orange. The ^{51}V NMR spectra of these solutions show that decavanadate ions are the only vanadium species with three characteristic peaks without any other vanadium signals (Figure 2). In contrast, when the pH was lowered, after spending more than 8 h at pH 11 to decolor and treated in the same way otherwise, the solutions showed much weaker orange color, and their ^{51}V NMR spectra showed many extra peaks in addition to those of decavanadates despite the favorable pH condition (not shown). In this case, the silicate shells function as a barrier for the fragmented vanadium species to recombine into decavanadate ions.

At this point, it is worthwhile to describe the NMR characteristics of the decavanadate ions. There are three different types of vanadium nuclei in the decavanadate ion, represented as V_I , V_{II} , and V_{III} in Figure 1. According to O'Donnell and Pope, these nuclei give rise to peaks at -420 , -500 , and -510 ppm, respectively, about

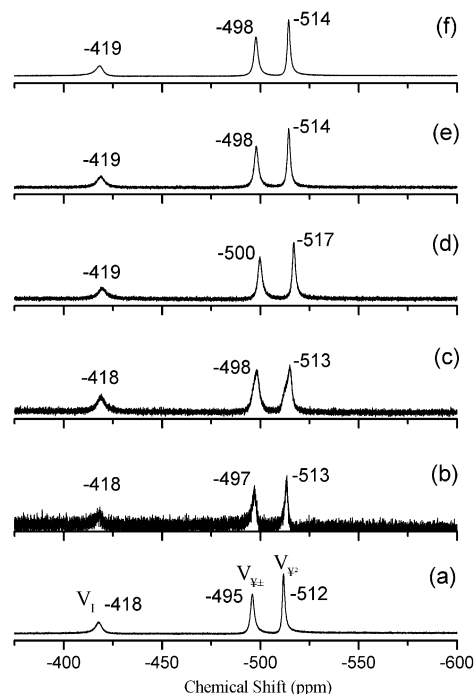


Figure 2. ^{51}V solution NMR spectra of decavanadate-silicate mixed solutions before gelation: (a) $V = 0.3$ M (pH = 4.5) reference solution, (b) VSi2.3, (c) VSi4.4, (d) VSi19, (e) VSi32, and (f) VSi48.

at pH 6.5, and at -425 , -504 , and -519 ppm, respectively, at pH 3.5, in an intensity ratio 1:2:2. The gradual upfield shifts with increasing acidity indicate that the $V_{10}O_{28}^{6-}$ is protonated stepwisely to $HV_{10}O_{28}^{5-}$ and to $H_2V_{10}O_{28}^{4-}$.¹⁶ From our own experiments on a $[V] = 0.3$ M solution, we have observed slightly different peak positions at -418 , -492 , and -508 ppm at pH 5.6, at -418 , -495 , and -512 at pH 4.5, and at -420 , -500 , and -518 at pH 3.5. The pre-gel solutions of pH 4.5 mentioned above gave peaks at -418 to -419 , -495 to -500 , and -512 to -517 ppm depending on the composition, similar to those of our pH 4.5 reference solution. (Figure 2)

Although the chemical shift data show some fluctuations with composition, one can find that the V nuclei with $V=O$ terminal oxo groups (V_{II} and V_{III} in Figure 1) show chemical shifts are upfield shifted by 1–5 ppm from the pH 4.5 reference, while the nuclei in the center of the cluster with bridging oxo ligands (V_I) show practically no change. This suggests that there are weak interactions between the decavanadate ions and the surrounding silica species, probably as hydrogen bonds of $V=O \cdots HO-Si$ type.

Upon aging at an elevated temperature of $86^\circ C$, the orange solutions turned into monolithic gels of different appearances depending on the vanadium content (Figure 3). While the reference vanadium-free VSi0.0 gel is colorless, characteristic for a silica gel, the other vanadium-containing samples are yellow (VSi2.3) or orange (VSi4.4–VSi48). In the latter group of high vanadium contents, the color intensity increases with the vanadium content. However, on the basis of our experience, the syntheses of these monolithic gels are increasingly more difficult with the increase of vanadium content. Although the reactions of up to VSi32 reproducibly produced monolithic gels, the synthesis of

(16) O'Donnell, S. E.; Pope, M. T. *J. Chem. Soc., Dalton Trans.* **1976**, 2290.

(17) Druskovich, D. M.; Kepert, D. L. *J. Chem. Soc., Dalton Trans.* **1975**, 947.

(18) Duraisamy, T.; Ramana, A.; Vittal, J. *J. Crystal Eng.* **2000**, *3*, 237. (b) Durif, P. A.; Averbuch-Pouchot, M. T.; Guitel, A. C. *Acta Crystallogr.* **1978**, *C43*, 197.



Figure 3. Decavanadate-incorporated silica gels of various vanadium concentrations after aging at 86 °C for 18 h. Samples are VSi0.0, VSi2.3, VSi4.4, VSi19, VSi32, and VSi48 from left to right.

VSi48 monolithic gel depends strongly on the process parameters, and the conditions described above appear to be the optimal. The delicate reaction conditions include kinetic controls. For example, when acid was added slightly too fast into the decavanadate–silicate mixture solution of pH 11, the products were opaque brown masses instead of the transparent monoliths, indicating the formation of V_2O_5 . Furthermore, the deep orange transparent monolithic gel of VSi48 turns into an opaque brown mass within one week when kept at 40 °C instead of at room temperature, an indication of the instability of this gel material. With these observations, we have concluded that VSi48 composition is the upper limit for monolithic gel formation in the present system, which is the highest among the related systems in the literature. In an analogous study using sol–gel reactions of alkoxide precursors, Dutoit et al. reported that they obtained homogeneous gels of up to 14.1 at. % of vanadium and that V_2O_5 crystallization occurred in a reaction of 22.1 at. % of vanadium. Their explanation is that the increasing vanadium content in the gel network causes continuous V–O–V connectivity formation that resulted in phase-segregation and crystallization of V_2O_5 .¹⁹

The solid state ^{51}V NMR spectra of all the orange-colored monolithic gels VSi2.3–VSi48 show three peaks at –427 to –428, –504 to –509, and –519 to –527 ppm with an intensity ratio of 1:2:2, characteristic for decavanadate ions (Figure 4). The peak positions show slight variations depending on the composition.

All of the three resonances of the decavanadate ions in the gel samples VSi2.3–VSi48 show upfield peak shifts by 5–15 ppm from those of the reference solution as well as the pre-gel solutions. This can be understood with the increased acidity of the matrix upon drying. However, like the solution NMR of the pre-gel materials, the vanadium nuclei at the periphery show concentration dependence in their peak positions while the central V_I appears constantly at –428 ppm within the chemical shift reading error of ± 1 ppm, indicating that there is an additional factor that affects the chemical shifts. This is most likely to be due to the bond formation of V–O–Si or V=O···H–O–Si type of the terminal V=O groups of V_{II} and V_{III} . The decavanadate ions in the gel samples

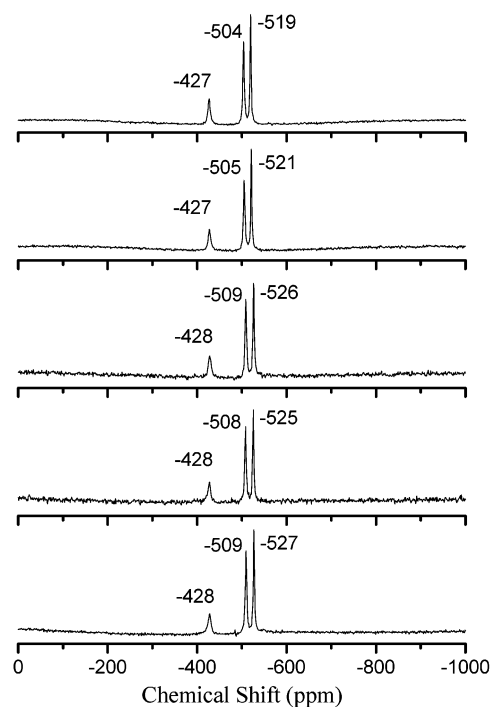


Figure 4. Solid state ^{51}V MAS NMR spectra of decavanadate-incorporated silica gels: (a) VSi2.3, (b) VSi4.4, (c) VSi19, (d) VSi32, and (e) VSi48.

show varying stability as a function of vanadium content. After being stored for a few weeks at room temperature, the VSi2.3 sample loses its orange color, and its solid-state NMR spectrum shows peaks at –525 and –572 ppm that can be assigned to $V_2O_7^{4-}$ and VO_4^{3-} surrounded by cations and/or bonded with silica species, respectively, instead of the peaks of decavanadate ion. Other samples do not show any noticeable changes by either visual inspection or solid state NMR. However, the observation on the VSi2.3 sample suggests that the decavanadate ions are kinetically stabilized and they are susceptible to changes into other vanadium species upon prolonged storage.

We have further characterized the monoliths with FT-IR spectroscopy. As shown in Figure 5, our reference VSi0.0 sample shows the characteristic peaks of a silica gel at 468 (Si–O–Si bending), 790 (Si–O–Si symmetric stretchings), 971 (Si–OH stretching), and 1105 and 1200 cm^{-1} (both asymmetric Si–O–Si stretching).^{22–24}

(19) Dutoit, D. C. M.; Schneider, M.; Baiker, A. *Chem. Mater.* **1996**, *8*, 734.

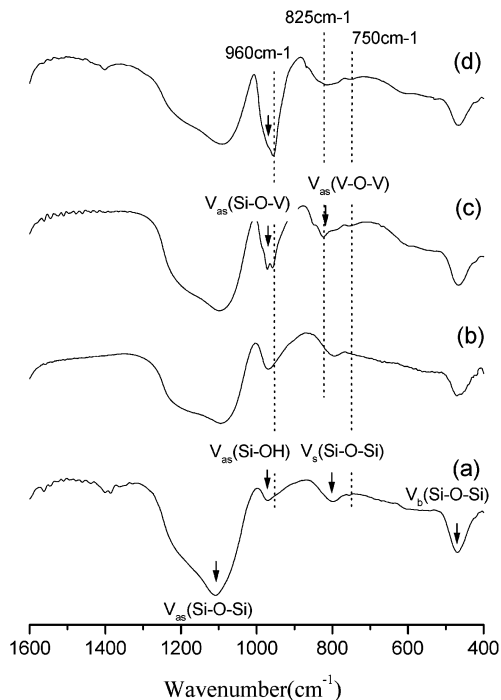


Figure 5. FT-IR spectra of decavanadate-incorporated silica gels: (a) VS i0.0 (reference), (b) VS i2.3, (c) VS i4.4, and (d) VS i19. Gels of higher vanadium contents are essentially the same as VS i19 except that the peak at 960 cm^{-1} is slightly enhanced; for clarity these are not shown.

The samples with greater vanadium contents than VS i2.3 show additional peaks at 750, 825, 960, and 980 cm^{-1} . The first two peaks are characteristic peaks for decavanadate ion,^{25,26} and the last one can be assigned to the V–O–Si or V=O···H–O–Si bonds.²² The 960 cm^{-1} peak is controversial. It is reported as one of the characteristic peaks of decavanadate ion.^{25,26} On the other hand, literature on vanadium-containing silica generally agree that this peak arises from the stretching of Si–O bonds perturbed by vanadium.^{27,28} Probably the two modes are superimposed in the present system. These peaks, especially those in 960–980 cm^{-1} range, grow in intensity with the vanadium content. On the other hand, the IR spectrum of the yellow VS i2.3 gel shows silica peaks only, probably because of the low vanadium content.

The thermal behaviors of the gel materials also reflect the nature of the vanadium species in the samples. In Figure 6, we show the TG data of the reference silica (VS i0.0) and the vanadium-containing samples (VS i2.3 and VS i4.4). All of the samples with vanadium contents

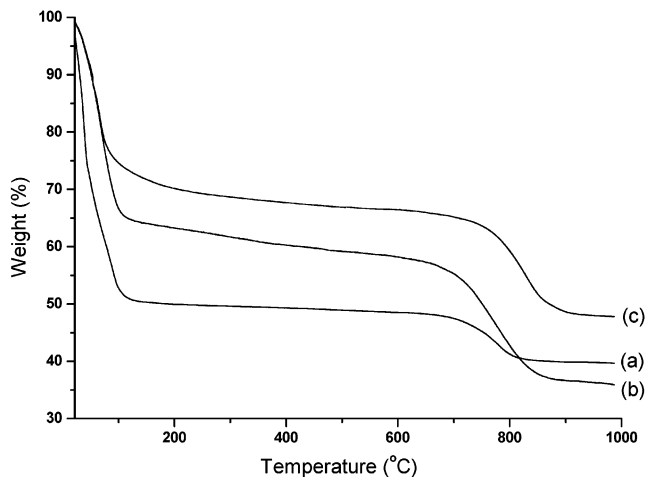


Figure 6. TG diagrams of decavanadate-incorporated silica gels: (a) VS i0.0 (reference), (b) VS i2.3, and (c) VS i32.

higher than that of VS i2.3 show similar TG patterns and only the data of VS i4.4 are shown in this figure. The reference silica shows two steps of weight loss at below 116 $^{\circ}\text{C}$ by 49% due to the water loss and at 650–700 $^{\circ}\text{C}$ by 8% due to the vaporization of Na_2O . The VS i2.3 sample also shows two weight loss steps at below 125 $^{\circ}\text{C}$ by 38% and at 650–700 $^{\circ}\text{C}$ by 28%, which also can be assigned to the losses of water and Na_2O , respectively. Between these steps, a gradual weight loss occurs by 7%, probably due to the loss of water molecules of various natures. VS i4.4 shows a pattern similar to that of VS i2.3 with weight losses at below 132 $^{\circ}\text{C}$ by 28%, at 132–708 $^{\circ}\text{C}$ by 8%, and at 708 $^{\circ}\text{C}$ by 21%. The water losses in these samples cannot be compared quantitatively because they may have started with different degrees of surface water contents. However, the general trend of decreasing water content with the increase of vanadium concentration appears to represent the nature of these materials. The water losses at the intermediate temperature regions in the vanadium-containing samples, which is absent in the reference silica, suggest that there are many OH^- groups that may be involved in the hydrogen bonds between the vanadium species and the silica matrixes. The larger Na_2O losses in the vanadium-containing samples are in accordance with the fact that the samples have been prepared with NaVO_3 . Also, the negative charges of the vanadate ions of any form require cations to balance their charges. Unfortunately, the gel materials turned out to be thermally unstable. Upon heating at 400 $^{\circ}\text{C}$ for 1 h, the X-ray amorphous materials became mixtures of $\text{Na}_{10}\text{V}_{24}\text{O}_{64}$, NaVO_3 , and an amorphous material.

The decavanadate ions in silica matrix of the present gel samples can be reduced by reducing agents. When a VS i32 gel sample was immersed in a 15% hydrazine hydrate solution the gel color changed from orange to dark green (Figure 7) in less than 1 h due to the reduction of vanadium ions from V^{5+} to V^{4+} .²⁹ The monolithic gel maintained its appearance while the green color diffused inwardly. This reduction process indicates that the silica network has diffusion pathways

(20) Kepert, D. L. *The Early Transition Metals*; Academic Press: London, 1972.

(21) Eckert, H.; Wachs, I. E. *J. Phys. Chem.* **1989**, *93*, 6796.

(22) Schraml-Marth, M.; Walther, K. L.; Wokaun, A.; Handy, B. E. Baiker, A. *J. Non-Cryst. Solids* **1992**, *143*, 93.

(23) Duran, A.; Serna, C.; Fornes, V.; Fernandez-Navarro, J. M. *J. Non-Cryst. Solids* **1986**, *82*, 69.

(24) Bertoluzza, A.; Fagnano, C.; Morelli, M. A.; Gottardi, V.; Guglielmi, M. *J. Non-Cryst. Solids* **1982**, *48*, 117.

(25) Day, V. W.; Klempner, W. G.; Maltbie, D. J. *J. Am. Chem. Soc.* **1987**, *109*, 9, 2991.

(26) Luca, V.; Hook, J. M. *Chem. Mater.* **1997**, *9*, 2731.

(27) Wie, D.; Wang, H.; Feng, X.; Chueh, W.-T.; Ravikovitch, P.; Lyubovskiy, M.; Li, C.; Takeguchi, T.; Haller, G. L. *J. Phys. Chem. B* **1999**, *103*, 2113.

(28) Dutoit, D. C.; Schneider, M.; Fabrizioli, P.; Baiker, A. *J. Mater. Chem.* **1997**, *7*, 271.

(29) Curran, M. D.; Poore, D. D.; Stiegman, A. E. *Chem. Mater.* **1998**, *10*, 3156.

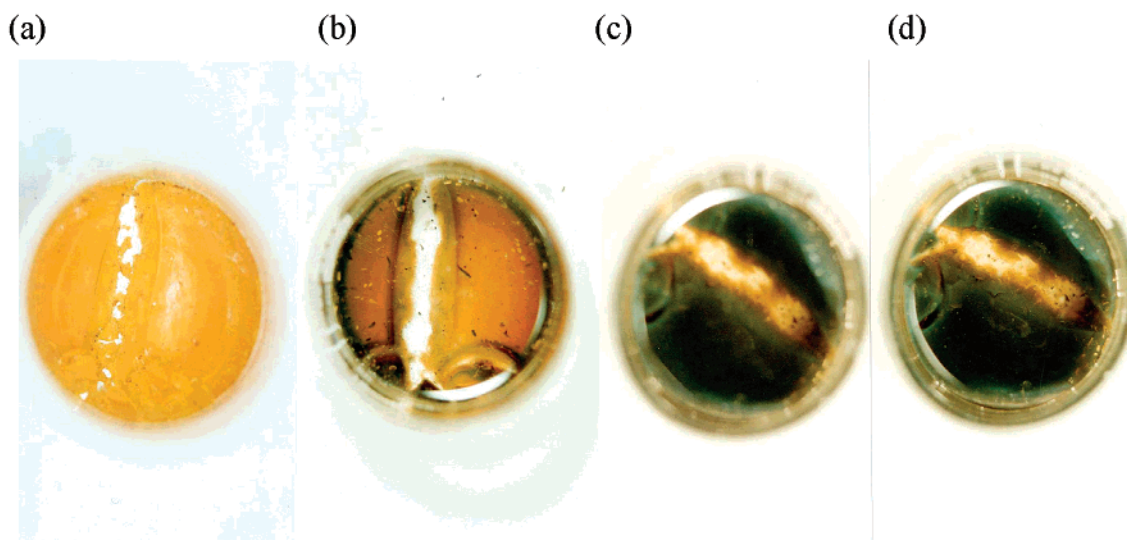


Figure 7. Reduction reaction of VSi₃₂ decavanadates-silica gel in a 15% hydrazine solution: (a) $t = 0$ min, (b) $t = 5$ min, (c) $t = 60$ min, and (d) $t = 24$ h.

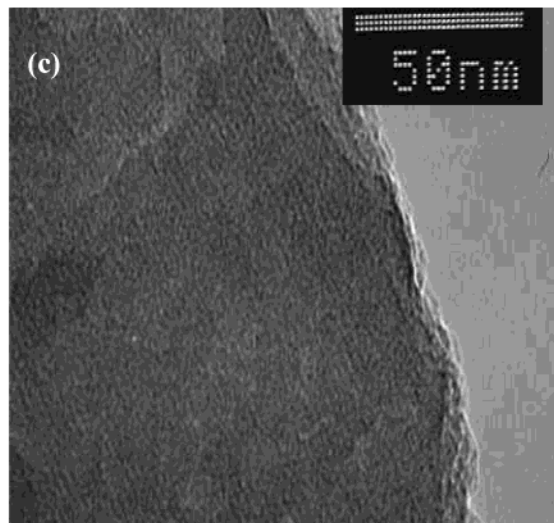
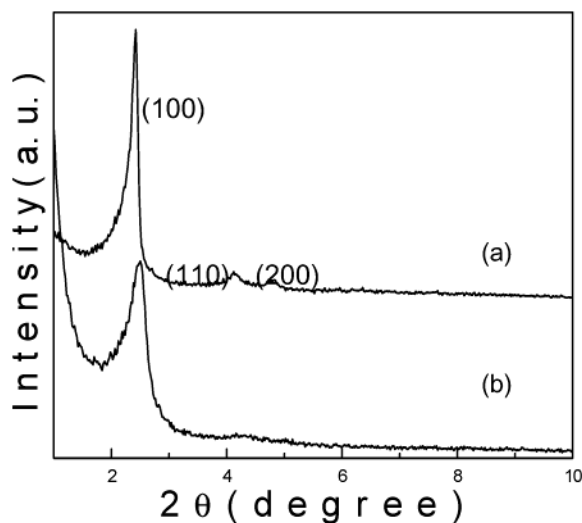


Figure 8. Mesostructured and mesoporous materials with vanadia-silica composite walls: (a) XRD pattern before photocalcination, and (b) XRD pattern and (c) TEM image after photocalcination.

for the hydrazine molecules to reach the decavanadate ions inside the matrix. Conversely, the catalytically active decavanadate ions inside the matrix are accessible by small molecules, a feature which may be useful for catalytic applications and fabrication of optical materials.

The above-assumed core-shell structure of decavanadate and silica prompted us to use it as a precursor for surfactant-templated mesostructured material synthesis. Stucky et al. have proposed that oligomeric silica species are formed during the formation of mesoporous silica.³⁰ We have also reported a synthesis of mesoporous titania by using titania sol solutions composed of 1–2-nm particles.³¹ Because the silica in the shell would behave in a manner similar to that of pure silica, we have adopted the procedure for MCM-41 synthesis using MTAB as a templating surfactant.³² The aged material

at pH 4.5 before calcination shows low-angle XRD peaks that can be indexed as (100), (110), and (200) for a 1D mesostructure with $a = 4.4$ nm (Figure 8a). Similar XRD patterns were obtained from the reactions of other pH conditions up to pH 8.0. Beyond this pH, there appears an additional peak at $d = 2.3$ nm due to the decavanadate-MTA complex.^{33,34} Unfortunately, these mesostructures are collapsed under the usual calcination conditions of 400 °C or higher for mesoporous silica synthesis, probably because of the thermal instability of the wall materials as described above. Therefore, we have used the photocalcination technique to remove the organics by using UV irradiation. The resultant XRD pattern and TEM image, in Figure 8b and c, respectively, both show that a 1D-hexagonal mesoporous material is obtained with $a = 4.0$ nm. These materials are pale yellow which indicates the incorporation of

(30) Firouzi, A.; Kumar, D.; Bull, L. M.; Besier, T.; Sieger, P.; Huo, Q.; Walker, S. A.; Zasadzinski, J. A.; Glinka, C.; Nicol, J.; Margolese, D.; Stucky, G. D.; Chmelka, B. F. *Science* **1995**, *267*, 1138.

(31) Hwang, Y.-K.; Lee, K.-C.; Kwon, Y.-U. *Chem. Commun.* **2001**, 1738.

(32) Lin, H.-P.; Cheng, S.; Mou, C.-Y. *Microporous Mater.* **1997**, *10*, 111.

(33) Stein, A.; Fendorf, M.; Jarvie, T. P.; Mueller, K. T.; Benesi, A. J.; Mallouk, T. E. *Chem. Mater.* **1995**, *7*, 304.

(34) Janauer, G. G.; Doble, A. D.; Zavalij, P. Y.; Whittingham, M. S. *Chem. Mater.* **1997**, *9*, 647.

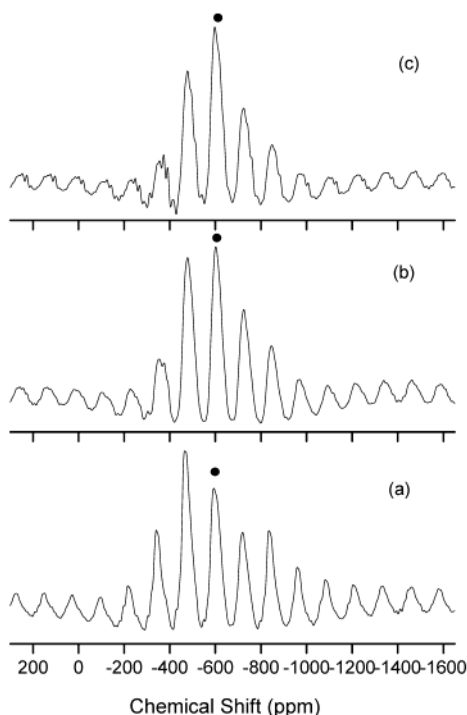


Figure 9. Solid state ^{51}V MAS NMR spectra of mesostructured and mesoporous materials with vanadia-silica composite walls prepared at various pH levels before photocalcination: (a) pH 4.5, (b) pH 6.0, and (c) pH 8.0. The circles represent center peaks.

polymeric vanadates in the silica wall. FT-IR spectroscopy shows the characteristic strong $\text{V}=\text{O}$ bonds vibration at 960 cm^{-1} . However, the IR spectrum also shows peaks at $2850\text{--}3000\text{ cm}^{-1}$ due to some residual organic materials, which prohibits reproducible characterization of the mesoprosity of this material.

Solid state ^{51}V MAS spectra of the aged material at pH 4.5 before photocalcination (Figure 9a) shows a broad center peak near -600 ppm flanked with many spinning sidebands. The broad peaks of the MAS spectra demonstrate the inhomogeneity of bond lengths and angles of the vanadium. As the gelation pH is higher, the spectrum pattern gets more symmetric in terms of chemical shift anisotropy, however, the center peaks have the same chemical shift within the experimental error range. Static echo spectra (not shown) also confirm that the spectrum pattern of chemical shift anisotropy is more symmetric for the higher pH sample, indicating

more deviation of the vanadium bonding symmetry from a cylindrical one. The chemical shifts of the MTAB surfactant-templated mesoporous sample are upfield shifted compared with those of the sample without the surfactant, and similar to the one observed from the five-coordinated $\text{V}(\text{V})$ in ref 35. This strongly suggests that decavanadate ions disintegrate to five-coordinated oxo-vanadate, partially polymerized, resulting in pale yellow color. Various chemical bonding of the oxygens of the oxo-vanadates with surrounding species such as silicate, Na^+ , Br^+ , H^+ , and possibly MTA ions, causes inhomogeneous chemical coordination states resulting in inhomogeneous line broadening of the MAS peaks. The symmetry change of the vanadium with pH variation implies that the chemical bonding with proton plays a major role for it.

Conclusions

In this study, we have shown that the pH-sensitive decavanadate ions can be kinetically stabilized by silicate ions even at high pH conditions, and that the resulting decavanadate-silica composite can be further processed into monolithic gels of record-breaking high vanadium contents and mesostructured and mesoporous materials with vanadia-silica walls. These data are the first demonstration of decavanadates-silica gel materials in which the POM ions are embedded without any significant structural modification. We also have synthesized mesostructured materials with vanadate-silica composite walls, although we have failed in obtaining pure mesoporous materials from this approach primarily because of the instability of the composite wall material.

With the simple principles used, the results of this paper can be easily adapted for other POMs and extended to incorporate various POMs into porous solid matrixes in the forms of gels or mesoporous materials for developing new catalyst materials.

Acknowledgment. Financial support of this research from the CNNC of SKKU and from the MOST through the KBSI(PG2213) are gratefully acknowledged. We also thank Prof. J. M. Kim at Ajou University for helpful discussion on the mesostructured materials.

CM034061I

(35) Das, N.; Eckert, H.; Hu, H.; Wachs, I. E.; Walzer, J. F.; Feher, F. J. *J. Phys. Chem.* **1993**, *97*, 8240.